Journal of
Synchrotron Radiation

ISSN 0909-0495

Received 25 October 2005
Accepted 25 August 2006

ASAXS, SAXS and SANS investigations of vulcanized elastomers filled with carbon black

Isabelle Morfin,[a]* Françoise Ehrburger-Dolle,[a] Isabelle Grillo,[b] Frédéric Livet[c] and Françoise Bley[c]

[a]Laboratoire de Spectrométrie Physique (UMR 5588 CNRS-UJF), BP 87, 38402 Saint-Martin d'Hères CEDEX, France, [b]Institut Laue-Langevin, 6 rue Jules Horowitz, BP 156, 38042 Grenoble CEDEX 9, France, and [c]Laboratoire de Thermodynamique et Physico-Chimie Métallurgiques (UMR 5614 CNRS-UJF-INPG), BP 75, 38402 Saint-Martin d'Hères CEDEX, France.
E-mail: isabelle.morfin@ujf-grenoble.fr

Small-angle X-ray scattering (SAXS) performed down to small q values ($q \leq 10^{-3}$ Å^{-1}) is a powerful method for investigating the arrangement of filler aggregates in filled elastomers under uniaxial strain. Meanwhile, for vulcanized samples, zinc oxide is used as an additive. Owing to their high contrast, the ZnO particles remaining in the manufactured composite are strong X-ray scatterers. In the low-q domain, their scattering hides that of filler aggregates (carbon black, pyrogenic silica) and must be quantified in order to be suppressed. To this end, anomalous SAXS (ASAXS) and small-angle neutron scattering (SANS) have been performed. It is shown that ASAXS measurements can be performed down to small q values ($q \leq 10^{-3}$ Å^{-1}). Therefore ASAXS is well adapted to separate the contributions of ZnO and filler scattering. For neutron scattering the contrast of the ZnO particles is similar to that of carbon. Because the amount of ZnO is much smaller than that of filler, ZnO scattering can be neglected. Owing to multiple scattering effects, however, SANS can only be used for very thin samples (less than about 0.25 mm). It is shown that, providing multiple scattering is avoided, ASAXS and SANS yield similar scattering curves for the filler aggregates.

Keywords: ASAXS; SAXS; SANS; polymer networks.

1. Introduction

The dispersion of solid particles (filler) in polymers, elastomers or rubber strongly modifies the physical properties of the resulting filler-matrix composite. Improvement of the mechanical properties (reinforcement) has been widely investigated but its mechanism is still not fully understood (Bokobza & Rapoport, 2002). Recent progress has been made by examining the role of the long-range structure of the filler network in theoretical approaches (Klüppel, 2003) and, in experiments, by carrying out small-angle scattering (SAS) measurements (Rharbi *et al.*, 1999; Westermann *et al.*, 1999, 2001). Recently, small-angle X-ray scattering (SAXS) measurements have been performed (Ehrburger-Dolle *et al.*, 2003) on several elastomers filled with carbon black or pyrogenic silicas. Uniaxial elongation of the samples may yield an anisotropic scattering characterized by a butterfly shape (Rharbi *et al.*, 1999) in the SAXS image, except for the series of cross-linked elastomers filled with carbon black. For the latter also, the shape of the SAXS curve suggests a stronger interpenetration of the carbon black aggregates than for uncross-linked matrices. A previous investigation (Ehrburger-Dolle *et al.*, 2001) of carbon-black-filled polyethylene led to a similar conclusion. Since these two features (degree of interpenetration of aggregates and deformation or not of the aggregate network) are also related to the shape of the stress–strain curve, SAXS measurements are essential to characterize a given composite material and to work out a realistic model that describes its mechanical properties.

The most common cross-linking method used for natural rubber or styrene-butadiene rubber is vulcanization, which involves addition of zinc oxide particles usually of micrometric or submicrometric sizes. As will be shown below, these ZnO particles produce strong X-ray scattering, especially at very small angles ($q < 0.005$ Å^{-1}), as a result of the large electron density of Zn as compared with that of carbon. This effect prevents a correct measurement of the very small-angle scattering related to the filler aggregates. Our goal was to discriminate experimentally between scattering resulting from carbon black aggregates and from ZnO particles. There are essentially two experimental methods to be considered for this purpose: anomalous small-angle X-ray scattering (ASAXS) and small-angle neutron scattering (SANS).

ASAXS, which is based on the anomalous variation of a scattering factor near an absorption edge, has been increasingly used over the last few years in materials science to study metal-supported catalysts, metastable precipitates in alloys, and polyelectrolyte systems (Haubold *et al.*, 1996, 1997; Polizzi *et al.*, 2002; Goerigk *et al.*, 2003; Fratzl, 2003; Guilleaume *et al.*, 2002). Anomalous ultra-SAXS has also been used to study materials under deformation (Lofaj *et al.*, 2001). The *K*-edge of Zn is located at an energy (9661 eV) which is experimentally accessible using synchrotron sources. The variation of the ASAXS ZnO contrast can be used to separate the contribution of zinc oxide from that of carbon.

In SANS, the scattering-length densities of carbon black and ZnO are similar. As the ZnO concentration is small, Belina *et al.* (2003) could obtain the intensity scattered by carbon black.

The aim of the present work was twofold: first, to separate the scattering of carbon black (C) from that of ZnO particles by means of ASAXS measurements, and, second, to compare the carbon black neutron scattering with ASAXS results.

Table 1
Description of the samples.

Values of the transmissions T_r (SANS measurements) discussed in §3.3 are also given.

		Filler content				
Sample	Matrix	phr	φ	Cross-linking method	Thickness (mm)	T_r (SANS)
S1	SBR	0	0	Vulcanization (ZnO)	0.56	0.64 (λ = 10 Å) 0.72 (λ = 5 Å)
S2	SBR	20	0.10	Vulcanization (ZnO)	0.51	0.47 (λ = 10 Å) 0.74 (λ = 5 Å)
S3	SBR	40	0.18	Vulcanization (ZnO)	0.63	0.30 (λ = 10 Å) 0.67 (λ = 5 Å)
S3μ					0.001	1.0 (λ = 10 Å) 1.0 (λ = 5 Å)
S4	SBR	45	0.20	Vulcanization (ZnO)	0.50	0.37 (λ = 10 Å) 0.72 (λ = 5 Å)
S0	SBR	40	0.18	Dicumyl peroxide	0.25	0.63 (λ = 10 Å) 0.84 (λ = 5 Å)
S5	EPR	45	0.20	Dicumyl peroxide	0.85	0.09 (λ = 10 Å) 0.48 (λ = 5 Å)

2. Experimental

2.1. Sample preparation

The elastomer matrix is styrene–butadiene rubber (SBR) containing 23.5% styrene (Duradene 706, Bridgestone/Firestone). The glass transition temperature measured by differential scanning calorimetry is 220 K. Carbon black N330 (Sid Richardson) used as filler is mixed with the matrix and the vulcanization agents in a miniature internal mixer, Haake Rheocord 90, and molded into sheets (thickness 0.5–0.8 mm). The amount of carbon black, expressed as parts of carbon black per hundred parts of rubber (phr), is 20 phr (sample S2), 40 phr (sample S3) and 45 phr (sample S4). The corresponding volume fractions φ are close to 0.10, 0.18 and 0.20, respectively. For sample S2, φ is slightly below the threshold φ^* (close to 0.11), above which a connected network of aggregates is formed. Sample S1 consists of vulcanized SBR, without carbon black. For all samples the amount of ZnO in the vulcanization formulation (ASTM D3191) is 3 phr. In order to examine a possible effect of multiple scattering in SANS, a thin sheet (S3μ) of sample S3 ($t \simeq 1$ μm) has been prepared by cryomicrotomy. For the reference sample (S0) without ZnO, cross-linking of SBR was achieved by means of dicumyl peroxide (2% *w*/*w* and no ZnO in the formulation). S0 contains the same amount (40 phr) of the same carbon black as sample S3. Its thickness is much smaller (t = 0.25 mm). Sample S5 consists of an ethylene–propylene rubber (EPR) matrix cross-linked also by means of dicumyl peroxide and containing 45 phr of the same carbon black. For S5, mixing of carbon black and rubber was achieved by means of a two-roll mill. Samples are listed in Table 1.

2.2. ASAXS measurements

Anomalous very small-angle scattering has been performed on the French-CRG beamline D2AM at ESRF (Simon *et al.*, 1997). A specific set-up (Livet *et al.*, 2003) allows measurements at very small angles to be performed: a 300 μm × 300 μm beam size was selected by means of carefully polished slits; a cross-shaped beam stop made of 300 μm Pt wires was used and the sample-to-detector distance was 2.1 m. The CCD camera with an X-ray-to-visible-light conversion taper has a 45 μm pixel size. Seven energies have been used: at 2, 5, 10, 20, 40 and 80 eV below the Zn *K*-edge (9661 eV) and one far from the Zn *K*-edge, at 7900 eV. The beam displacement on the sample is less than 50 μm during the energy scan, near the edge. After dark-current correction and radial averaging, data have been corrected for incoming beam intensity and sample transmission. An empirical constant background must be subtracted or added in order to take into account fluctuations of the dark current level and occurrence of resonant Raman scattering. Intensities have been calibrated within the same relative units by using samples without anomalous scattering.

2.3. SANS measurements

SANS experiments were performed on the instrument D11 at the Institut Laue Langevin (Grenoble). The sample-to-detector distances were D = 35.5 m (collimation = 40.5 m), 15.0 m (collimation = 16.5 m), and 5.0 m and 1 m (collimation = 8.0 m for both distances). The diameter of the diaphragm in front of the sample was equal to 8 mm for thick samples and 2 mm for the S3μ sample. To obtain a broad q-range, two wavelengths (λ = 10 and 5 Å) were used. The overall q-range was 10^{-3} to 10^{-1} Å^{-1}. Transmission of the samples was measured at D = 5 m for λ = 5 Å and D = 35.5 m for λ = 10 Å. In order to check for multiple-scattering effects, a series of measurements were also performed on the instrument D22 with λ = 20 Å for sample S3. Raw data were corrected for

electronic background and empty cell and normalized in absolute scale with water using standard ILL software (Lindner, 2002).

3. Experimental results

3.1. Evidence of the presence of ZnO particles in vulcanized rubber

The presence of ZnO particles in vulcanized composites is clearly shown on the scanning electron microscopy (SEM) picture (Fig. 1) and by X-ray microanalysis. The SAXS curve obtained for ZnO particles dispersed in the vulcanized SBR matrix without carbon black (sample S1) is plotted in Fig. 2. The downturn of the scattering curve ($\sim 10^{-3}$ Å^{-1}), an indication of the approach of the Guinier domain, confirms the micrometric size of the particles suggested by the SEM picture. For $q > 0.003$ Å^{-1}, one observes the Porod domain ($I \propto q^{-4}$).

The two samples (S4 and S5) filled with carbon black show very similar scattering for $q > 0.004$ Å^{-1}; at lower q values the extra intensity measured for the vulcanized sample (S4) as compared with that of sample S5 clearly results from the scattering of ZnO particles. It follows that fitting the S4 curve to a power law would have no physical meaning.

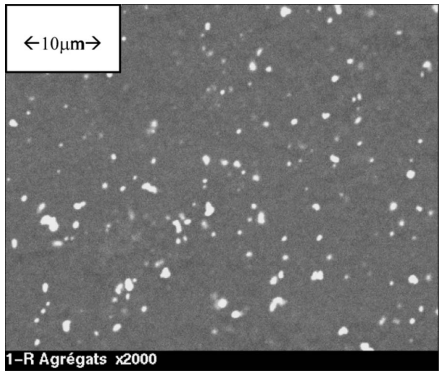

Figure 1
SEM image of sample S3. ZnO particles appear as white spots.

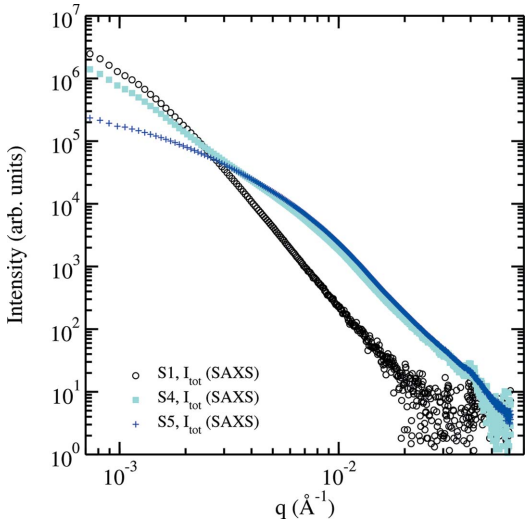

Figure 2
Small-angle X-ray scattering (7900 eV) by samples S1 and S4 containing ZnO and sample S5 (without ZnO).

3.2. ASAXS measurements

3.2.1. Contrast. Fig. 3(*a*) shows an example of scattering curves $I(q, E)$ measured at different energies E for a vulcanized sample (S1) containing the amount of ZnO particles necessary for the elastomer vulcanization. The anomalous effect is clearly seen. Addition of carbon black in the elastomer (sample S4) does not hide the anomalous effect of ZnO (Fig. 3*b*).

For vulcanized samples containing carbon black, $I(q, E)$ can be written as follows,

$$I(q, E) \propto I_{\mathrm{ZnZn}}(q, E) + I_{\mathrm{CC}}(q) + I_{\mathrm{ZnC}}(q, E) \qquad (1)$$

with

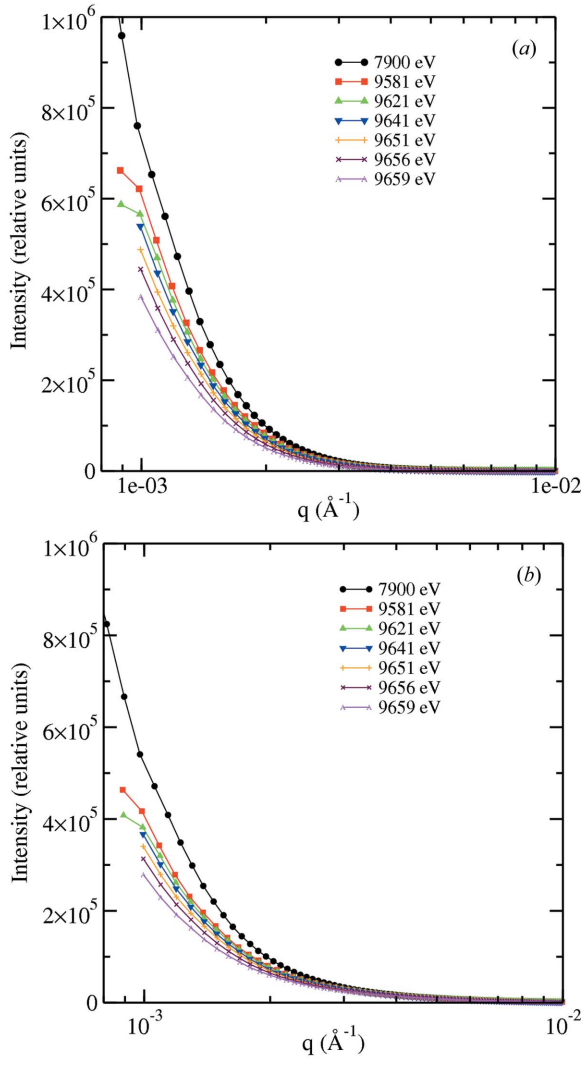

Figure 3
Intensity curves measured at the different energies for (*a*) sample S1 and (*b*) sample S4.

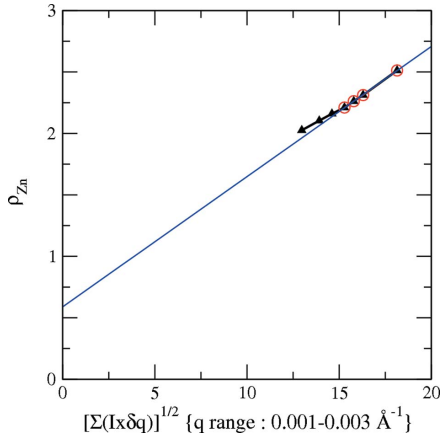

Figure 4
Correction of ρ_Z: the energy corresponding to each point varies between 9659 eV and 7900 eV. The equation of the fit is $\rho_{Zn} = 0.588(\pm 0.021) + 0.106(\pm 0.001)\{\Sigma[I(q)\,\delta q]\}^{1/2}$.

$$I_{ZnZn}(q, E) = \left[\rho_{Zn}(E) - \rho_P\right]^2 S_{ZnZn}(q), \tag{1a}$$

$$I_{CC}(q) = \left(\rho_C - \rho_P\right)^2 S_{CC}(q), \tag{1b}$$

$$I_{ZnC}(q, E) = \left(\rho_C - \rho_P\right)\left[\rho_{Zn}(E) - \rho_P\right] S_{ZnC}(q), \tag{1c}$$

where S_{ZnZn} is the structure factor of ZnO particles, S_{CC} is the structure factor of carbon black, S_{ZnC} is the cross term, and ρ_P, ρ_C and $\rho_{Zn}(E)$ are the electronic densities of polymer, carbon black and ZnO, respectively. The elastomer matrix is taken as the reference because its scattering is small compared with that of ZnO or carbon black.

The first step consists of calculating the anomalous electronic density by using the data obtained for sample S1 containing only ZnO but no carbon black, for which

$$I(q, E) = I_{ZnZn}(q, E) = \left[\rho_{Zn}(E) - \rho_P\right]^2 S_{ZnZn}(q). \tag{1d}$$

Near the Zn absorption K-edge, the electronic density of ZnO varies with energy, according to the anomalous dispersion corrections. Below the Zn edge, the imaginary anomalous dispersion factor $f''(E)$ is small and can be neglected. It follows that

$$\rho_{ZnO}(E) = \frac{f_O^0 + f_{Zn}^0 + f'_{Zn}(E)}{A}\,\mu, \tag{1e}$$

where f_i^0 is the atomic scattering factor (= Z at small angles), $f'_{Zn}(E)$ is the real anomalous dispersion factor, A is the molar mass and μ is the specific gravity of the ZnO particles. For the sake of clarity, $\rho_{ZnO}(E)$ will be written as $\rho_{Zn}(E)$. In order to improve the statistics, the intensity $I(q, E)$ will be replaced by an integration $\Sigma(I)$ over a narrow range of q values, $\delta q = 2 \times 10^{-3}$ Å^{-1}. $\rho_{Zn}(E)$ can be calculated from (1e) by using the value of the anomalous dispersion factors obtained from the tables of Cromer & Liberman (1970). Fig. 4 shows the variation of $\rho_{Zn}(E)$ as a function of $[\Sigma I(q)\,\delta q]^{1/2}$, which is linear, at least far from the edge, as expected by (1d). When approaching the edge, *i.e.* 2, 5 and 10 eV below the edge [small values of $\rho_{Zn}(E)$], the data depart from linearity as a result of the finite bandwidths of the monochromator and of the edge

Table 2
Contrast coefficients, after correction of the ZnO contrast close to the Zn edge.

The errors on $(\rho_{Zn} - \rho_P)^2$ and $(\rho_{Zn} - \rho_P)(\rho_C - \rho_P)$ are close to 008 and 004, respectively, but all errors are correlated. $(\rho_C - \rho_P)^2 = 0.113 \pm 0.014$ is independent of energy.

	E (eV)						
	7900	9581	9621	9641	9651	9656	9659
$(\rho_{Zn} - \rho_P)^2$	3.692	2.989	2.796	2.621	2.394	2.173	1.887
$(\rho_{Zn} - \rho_P)(\rho_C - \rho_P)$	0.646	0.581	0.563	0.545	0.521	0.496	0.462

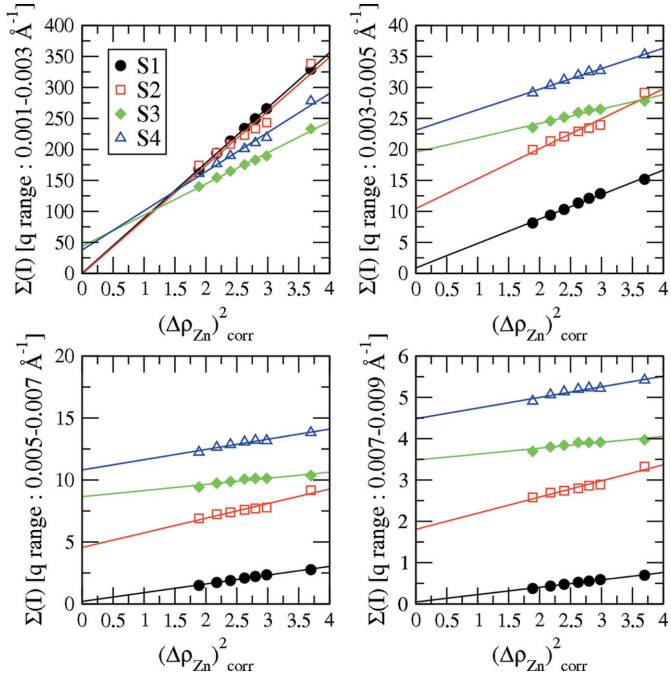

Figure 5
Dependence of the intensity (summed over $\delta q = 2 \times 10^{-3}$ Å^{-1}) on the ZnO-matrix-corrected contrast for the vulcanized samples containing increasing amounts of carbon black: S1 ($\varphi_{CB} = 0$), S2 ($\varphi_{CB} = 0.10$), S3 ($\varphi_{CB} = 0.18$), S4 ($\varphi_{CB} = 0.20$).

(Goerigk *et al.*, 2003). The corrected values $[\rho_{Zn}(E)]_{corr}$ of $\rho_{Zn}(E)$ are obtained from the fitting line plotted in Fig. 4 which also yields the electronic density of the polymer matrix, $\rho_P = 0.588$. The values of $(\rho_{Zn} - \rho_P)^2$ obtained by this method for each energy are collected in Table 2.

The electronic density of carbon, ρ_C, and, therefore, the contrast $(\Delta\rho_C)^2 = (\rho_C - \rho_P)^2 = 0.113$ are independent of energy in the investigated energy domain. The values of the energy-dependent term $(\rho_C - \rho_P)[\rho_{Zn}(E) - \rho_P]$ in (1c) are also given (Table 2).

Because the ZnO particles are large and because their volume fraction is small as compared with that of carbon black, the probability of interference between ZnO and carbon black scattering should be small. Under such circumstances (Polizzi *et al.*, 2002) the cross term can be neglected in (1). It follows that $I(q, E)$ or, as above, $[\Sigma(I)]$ is expected to vary linearly with $[\Delta\rho_{Zn}(E)]^2$. The curves obtained for the different samples are plotted in Fig. 5 at four different

q ranges for which the intensity is large enough to be significant.

The intercept of the curves at $(\Delta\rho_{Zn})^2 = 0$ with the vertical axis corresponds to the contribution of $I_{CC}(q)$ at a given q value. The slope of each curve is related to the contribution of $I_{ZnZn}(E, q)$ at a given q. As mentioned above, for samples containing carbon black, a significant contribution of the cross term would yield a departure from linearity, not observed here. The regression lines are obtained by using the six energies close to the edge, for which the position of the beam does not change. For E = 7900 eV, the irradiated part of the sample is no longer the same since the beam position has slightly changed. The regression coefficient r^2 ranges from 0.99 to 0.98 for all curves in the three first figures where the intensity is large enough. For the fourth, the quality of the linear fit is poorer for all curves, as a result of the low values of the intensity. Thus, it is likely that the influence of the cross term is weak as will be seen in the next paragraph. Data points shown on Fig. 5 include those obtained at 7900 eV, corresponding to the largest value of $[\Delta\rho_{Zn}(E)]^2$. These measurements were performed in order to improve the quality of the contrast matrix. Meanwhile it appears (Fig. 5) that, in some cases, the experimental points do not align very well with the data obtained at higher energies. This feature suggests that the increase of contrast is not large enough to balance the loss of accuracy related to the beam position change due to a large energy variation.

3.2.2. Partial structure factors. Once the contrast values are known, the three partial structure factors $S_{ZnZn}(q)$, $S_{CC}(q)$ and $S_{ZnC}(q)$ are extracted by least-square calculations from the linear system of equations (1*a*)–(1*c*).

Fig. 6 shows the resulting structure factors calculated for sample S4 with all three terms and without the cross term S_{ZnC}. It is obvious that the inversion of the matrix containing the three terms is not reliable. The results only reveal an amplification of statistical errors. Cenedese *et al.* (1984) have already shown that the reliability of the solution is very low when the matrix is ill-conditioned. This is the case when the cross term is taken into account. Later, Lyon & Simon (1987) indicated that the cross term can be extracted only if measurements are performed at two different edges. Such experiments, however, are not feasible in the case of ZnO. These two observations, along with evidences given by Fig. 5 on the one hand and size and volume fraction of ZnO particles on the other, allow one to assume that neglecting the cross term is relevant to the present systems.

In order to check further the validity of this assumption, the CC partial intensity $I_{CC}(q)$ in (1*b*) (neglecting the cross term) for sample S3 is compared with the intensity scattered by sample S0, containing the same amount of carbon black but no ZnO.

Fig. 7 shows that the two curves have the same shape and differ only by a proportionality factor. This feature suggests that neglecting the cross term, *i.e.* neglecting the interferences between scattering of carbon black and ZnO particles, does not modify S_{CC} significantly. It also provides evidence for the pertinence of the procedure for determining the carbon black structure factors S_{CC} obtained for samples S1 to S4 plotted in Fig. 8.

Meanwhile, the shape of the $S_{ZnZn}(q)$ curves obtained for these samples, also plotted in Fig. 8, seems to depend weakly on the amount of carbon black dispersed in the matrix. This feature suggests that neglecting the cross terms has a larger effect on the ZnZn partial structure factor than on the CC partial structure factor. As explained above, the cross term cannot be properly extracted in the present experiments. Therefore there is no other choice than disregarding it and checking, by SANS, the correctness of the carbon black structure factor S_{CC} obtained by ASAXS. The next paragraph is therefore devoted to the comparison of the S_{CC} curves with

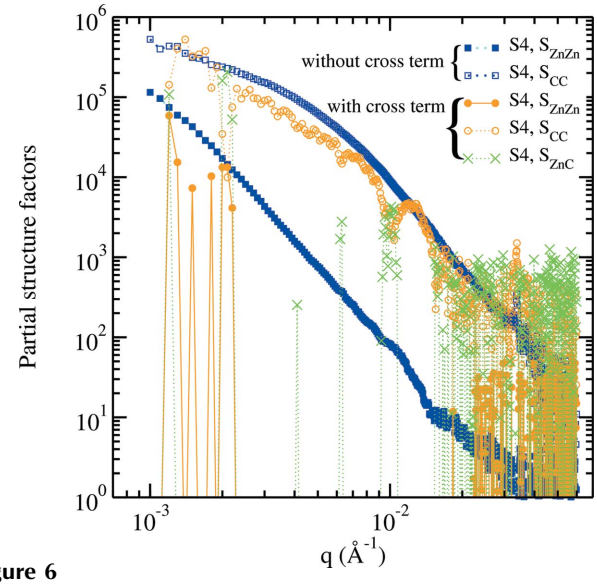

Figure 6
Partial structure factors for sample S4, calculated using the three functions or by neglecting the cross term.

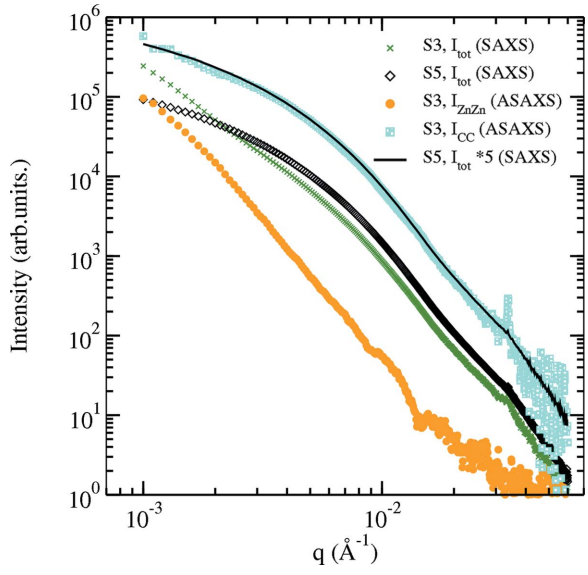

Figure 7
Comparison of reconstructed intensities at 9659 eV of sample S3 and sample S0 (without ZnO); the sharp peak observed near q = 0.03 Å^{-1} is due to noise.

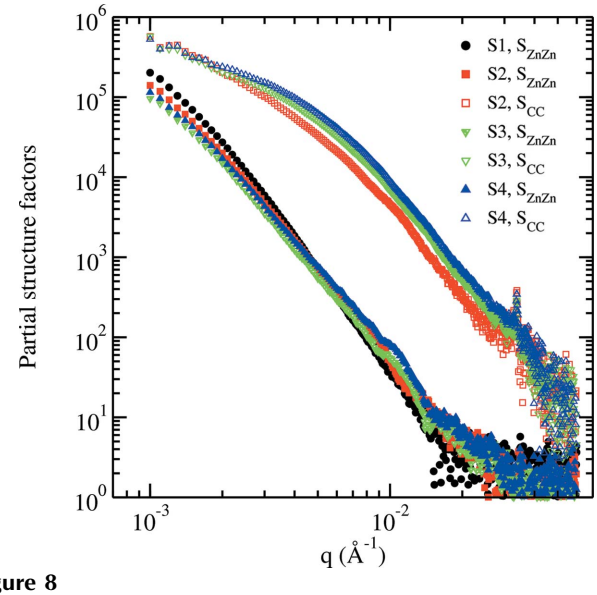

Figure 8
Partial structure factors S_{CC} and S_{ZnZn} for all samples containing ZnO (the cross term S_{ZnC} is neglected); the sharp peak observed near q = 0.03 Å^{-1} is due to noise.

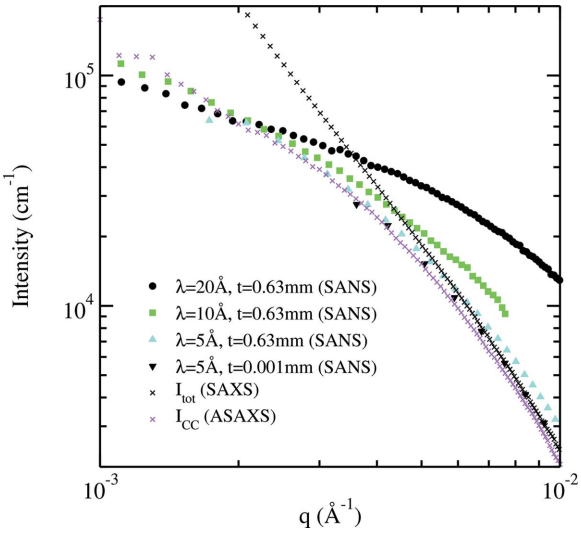

Figure 9
Multiple-scattering effects in SANS measurements: SANS curves measured for S3 at different wavelengths and two different thicknesses. (The ASAXS and SAXS curves are not normalized and have been shifted for overlapping the S3μ SANS curve.)

those obtained by SANS. Because a precise analysis of SAXS curves has already been made (Rieker *et al.*, 2000; Ehrburger-Dolle *et al.*, 2001), only the shape of the SANS curves will be compared, without further analysis.

3.3. SANS measurements and comparison with ASAXS

Fig. 9 shows the SANS curves obtained for sample S3 at three different wavelengths. The curves do not superimpose. This feature reveals multiple-scattering affects (Lindner, 2002) for this sample with a thickness t = 0.63 mm. For the very thin sample, S3μ (t = 1 μm), the intensity scattered for λ = 20 and 10 Å (low-q domain) was too small to be accurately measured. The curve obtained for this sample, with λ = 5 Å and D = 15 m (taking into account the uncertainty of the sample thickness), and that obtained for sample S3, under the same conditions, are almost superimposed. Above 0.0035 Å^{-1}, the SANS data obtained for S3μ are close to those obtained by SAXS and by ASAXS for S3. This set of curves shows that multiple scattering cannot be avoided for sample S3 (thickness = 0.63 mm) at λ = 10 Å, the wavelength needed to reach low q values. As a result, the SANS curve goes below the ASAXS curve for q < 0.002 Å^{-1}. In order to overcome the multiple-scattering problem, a thinner sample (t = 0.25 mm) was investigated. For this thinner sample, S0, which does not contain ZnO, the transmission T_r is 0.63 (λ = 10 Å) and 0.84 (λ = 5 Å).

Fig. 10 shows that the curves measured at 10 and 5 Å in the low-q domain are almost overlapping. It may be concluded that there is no multiple scattering for this sample. This figure also shows that SANS and SAXS curves overlap fairly well. It is also the case for the ASAXS curve obtained for sample S3 (also plotted in Fig. 9).

It has been shown earlier (Rieker *et al.*, 2000) that carbon black aggregates dispersed in polyethylene are not, or are only weakly, interpenetrated when the volume fraction is below or

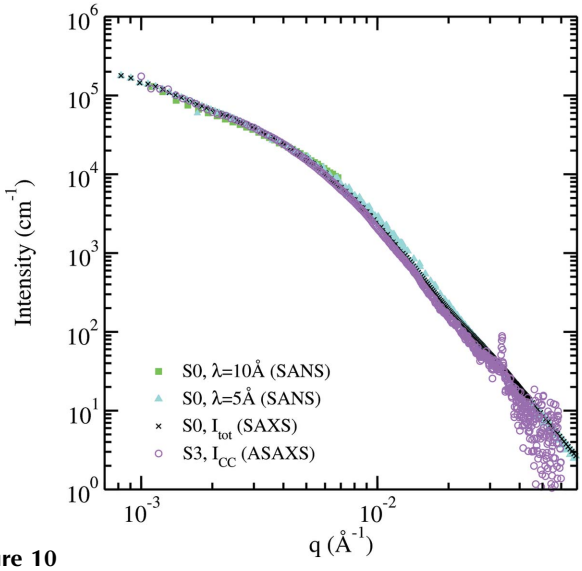

Figure 10
Comparison between SANS and SAXS curves obtained for sample S0 (t = 0.25 mm) cross linked with dicumyl peroxide (no ZnO) and the ASAXS curve obtained for sample S3 (t = 0.63 mm) containing the same amount of the same carbon black and ZnO.

close to the percolation threshold ($\varphi^* \simeq 0.11$). In this case a power-law domain resulting from the structure factor of fractal aggregates is observed in the low-q domain. The exponent, $-D_m$, yields the fractal dimension of the carbon black aggregates ($D_m \simeq 1.8$).

Fig. 11 indicates that the expected behavior is observed for the ASAXS curve obtained for sample S2 (φ = 0.10). Since multiple scattering occurs in this q-range, the SANS curve displays a smaller slope. For sample S4, filled with a large amount of carbon black (45 phr corresponding to φ close to 0.20, well above the percolation threshold), the shape of the ASAXS curve is similar to that of the SAXS curve obtained for sample S5 (EPR matrix cross-linked with dicumyl peroxide

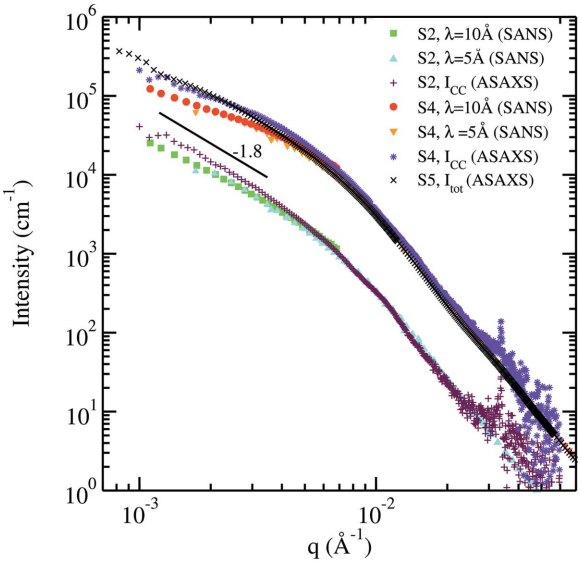

Figure 11
Comparison between ASAXS, SAXS and SANS curves obtained for samples S2 ($\varphi < \varphi^*$) and samples S4 and S5 ($\varphi > \varphi^*$).

containing the same amount of the same carbon black). Similarly to S2, multiple scattering induced a lower SANS intensity in the low-q domain. Sample S5 is much thicker (t = 0.85 mm) than sample S4 (t = 0.50 mm) and displays strong multiple scattering (SANS curve not shown).

4. Discussion

ASAXS experiments were undertaken in order to discriminate between the scattering of ZnO particles added for vulcanization and the scattering of carbon black aggregates that one is interested in. Analysis of the results shows that this goal is reached. We have verified that SANS yields curves that only result from carbon black aggregates. The major problem with SANS experiments on carbon-black-filled elastomers is multiple scattering. This effect has been investigated in detail above, by changing the neutron wavelength and the sample thicknesses. Thus, for most samples, analysis of SANS data compounded by multiple scattering (Allen *et al.*, 2001; Mazumder *et al.*, 1998) should be carried out. This procedure was not used here because it goes beyond the scope of the present work. Our results indicate that multiple scattering is avoided when the sample thickness is smaller than about 0.25 mm for λ = 10 Å. When this condition is fulfilled, SANS and ASAXS curves are the same. This feature proves the merits of the ASAXS analysis performed above and validates *a posteriori* omission of the cross terms. Furthermore, the comparison between ASAXS, SAXS and SANS curves obtained for samples with or without ZnO suggests that, in SAXS experiments, multiple scattering in the low-q domain is almost negligible.

The ultimate goal of the experiments described here was to be able to investigate the modification of the arrangement of carbon black aggregates during uniaxial stretching in vulcanized composite, similar to what was performed on composites containing no ZnO. To this end, SANS measurements are faster and easier than ASAXS measurements. However, owing to the problem of multiple scattering, either multiple scattering has to be taken into account in the data analysis or ASAXS can be used. ASAXS may have to be used if the sample thickness cannot be made smaller. It was shown that an occurrence of an anisotropy in the SAXS curves (butterfly pattern) is related to a particular mechanical behavior. In order to check whether this feature is observed with SANS, even if multiple scattering cannot be avoided, all samples were also measured at 100% elongation (*i.e.* the stretch ratio is equal to 2). The results (not shown here) indicate that (i) all stretched (100%) uncross-linked composites display a SANS butterfly pattern, as they do for SAXS; (ii) all stretched (100%) cross-linked samples, *i.e.* those cross-linked with dicumyl peroxide investigated earlier by SAXS and those investigated now by SAXS and SANS, do not display butterfly patterns.

This latter observation is different from that reported by Belina *et al.* (2003) for a filled vulcanized polyisoprene for which a butterfly pattern has been observed. Meanwhile, the stretch ratio (equal to 2.5) and the amount of filler (φ = 0.22) were larger. Also, the type of carbon black (N339) was different. It is worth mentioning, however, that we also observed butterfly patterns for cross-linked matrices filled by pyrogenic silicas (Ehrburger-Dolle *et al.*, 2003). For these samples also, the stress–strain curves display a yield point or a wide plateau.

The above discussion confirms that information about the arrangement of aggregates in the matrix and about the way the network changes its shape during uniaxial stretching is essential to explain the macroscopic mechanical behavior. It appears that these features are very sensitive to several parameters which need to be clearly identified in order to find general equations describing the mechanical behavior. Thus, for vulcanized samples which are close to industrially relevant samples, it is necessary to be able to discriminate between ZnO and carbon black scattering.

5. Conclusion

The present work has shown that ASAXS measurements can be successfully performed down to small q-values (10^{-3} Å^{-1}). It follows that ASAXS is well adapted for investigating the arrangement of carbon black aggregates in vulcanized elastomer, containing ZnO. SANS experiments have been performed on the same samples. However, unlike SAXS, the occurrence of multiple scattering in samples usually studied in mechanical measurements (thickness ranging between 0.5 and 1 mm) is a major drawback requesting special methods of analysis. For such industrial samples, ASAXS is a unique method for investigating the arrangement of the carbon black aggregates in the elastomeric matrix under uniaxial strain. For vulcanized samples that can be made thin (less than about 0.25 mm), SANS is the most convenient method for the above purpose.

We are grateful to the ERSF, Grenoble, for access to the French CRG beamline D2AM and the help of its technical staff, J.-F. Berar, N. Boudet, B. Caillot and S. Arnaud. We also thank the ILL, Grenoble, for beam time allocation.

References

Allen, A. J., Ilavsky, J., Long, G. G., Wallace, J. S., Berndt, C. C. & Herman, H. (2001). *Acta Mater.* **49**, 1661–1675.
Belina, G., Urban, V., Straube, E., Pyckhout-Hintzen, W., Klüppel, M. & Heinrich, G. (2003). *Macromol. Symp.* **200**, 121–128.
Bokobza, L. & Rapoport, O. (2002). *J. Appl. Polym. Sci.* **85**, 2301–2316.
Cenedese, P., Bley, F. & Lefebvre, S. (1984). *Acta Cryst.* A**40**, 228–240.
Cromer, D. T. & Liberman, D. (1970). *J. Chem. Phys.* **53**, 1891–1898.
Ehrburger-Dolle, F., Bley, F., Geissler, E., Livet, F., Morfin, I. & Rochas, C. (2003). *Macromol. Symp.* **200**, 157–167.
Ehrburger-Dolle, F., Hindermann-Bischoff, M., Geissler, E., Rochas, C., Bley, F. & Livet, F. (2001). *Langmuir*, **17**, 329–334.
Fratzl, P. (2003). *J. Appl. Cryst.* **36**, 397–404.
Goerigk, G., Haubolb, H.-G., Lyon, O. & Simon, J.-P. (2003). *J. Appl. Cryst.* **36**, 425–429.
Guilleaume, B., Blaul, J., Ballauff, M., Wittemann, M., Rehahn, M. & Goerigk, G. (2002). *Eur. Phys. E*, **8**, 299–309.
Haubold, H.-G., Wang, X. H., Goerigk, G. & Schilling, W. (1997). *J. Appl. Cryst.* **30**, 653–658.
Haubold, H.-G., Wang, X. H., Jungbluth, H., Goerigk, G. & Schilling, W. (1996). *J. Mol. Struct.* **383**, 283–289.
Klüppel, M. (2003). *Adv. Polym. Sci.* **164**, 1–86.
Lindner, P. (2002). *Neutrons, X-rays and Light: Scattering Methods Applied to Soft Condensed Matter*, edited by P. Lindner and Th. Zemb, pp. 23–48. Amsterdam: Elsevier Science.
Livet, F., Bley, F., Ehrburger-Dolle, F., Geissler, E., Leboloc'h, D. & Schulli, T. (2003). *J. Appl. Cryst.* **36**, 774–777.
Lofaj, F., Long, G. G. & Jemian, P. (2001). *Ceram. Eng. Sci. Proc.* **22**, 167–174.
Lyon, O. & Simon, J. P. (1987). *Phys. Rev. B*, **35**, 5164–5174.
Mazumder, S., Jayaswal, B. & Sequira, A. (1998). *Physica B*, **241–243**, 1222–1224.
Polizzi, S., Riello, P., Goerigk, G. & Benedetti, A. (2002). *J. Synchrotron Rad.* **9**, 65–70.
Rharbi, Y., Cabane, B., Vacher, A., Joanicot, M. & Boué, F. (1999). *Europhys. Lett.* **46**, 472–478.
Rieker, T. P., Hindermann-Bischoff, M. & Ehrburger-Dolle, F. (2000). *Langmuir*, **16**, 5588–5592.
Simon, J. P., Arnaud, S., Bley, F., Berar, J. F., Caillot, B., Comparat, V., Geissler, E., de Geyer, A., Jeantey, P., Livet, F. & Okuda, H. (1997). *J. Appl. Cryst.* **30**, 900–904.
Westermann, S., Kreitschmann, M., Pyckhout-Hintzen, W., Richter, D., Straube, E., Farago, B. & Goerigk, G. (1999). *Macromolecules*, **32**, 5793–5802.
Westermann, S., Pyckhout-Hintzen, W., Richter, D., Straube, E., Egelhaaf, S. & May, R. (2001). *Macromolecules*, **34**, 2186–2194.